Solubilizing Mutations Used to Crystallize One CFTR Domain Attenuate the Trafficking and Channel Defects Caused by the Major Cystic Fibrosis Mutation

Luísa S. Pissarra,[1,5] Carlos M. Farinha,[1,2,5] Zhe Xu,[3] André Schmidt,[2] Patrick H. Thibodeau,[4,6] Zhiwei Cai,[3] Philip J. Thomas,[4] David N. Sheppard,[3] and Margarida D. Amaral[1,2,*]

[1]Department of Chemistry and Biochemistry, Faculty of Sciences, University of Lisboa, 1749-016 Lisboa, Portugal
[2]Centre of Human Genetics, National Institute of Health, 1649-016 Lisboa, Portugal
[3]Department of Physiology and Pharmacology, School of Medical Sciences, University of Bristol, BS8 1TD Bristol, United Kingdom
[4]Department of Physiology, University of Texas Southwestern Medical Center Dallas, TX 75390, USA
[5]These authors contributed equally to this work.
[6]Present address: Department of Cell Biology and Physiology, University of Pittsburgh School of Medicine, Pittsburgh, PA 15261, USA.
*Correspondence: mdamaral@fc.ul.pt

SUMMARY

Cystic fibrosis (CF) is caused by mutations in the CF transmembrane conductance regulator (CFTR) Cl⁻ channel. F508del, the most frequent CF-causing mutation, disrupts both the processing and function of CFTR. Recently, the crystal structure of the first nucleotide-binding domain of CFTR bearing F508del (F508del-NBD1) was elucidated. Although F508del-NBD1 shows only minor conformational changes relative to that of wild-type NBD1, additional mutations (F494N/Q637R or F429S/F494N/Q637R) were required for domain solubility and crystallization. Here we show that these solubilizing mutations in *cis* with F508del partially rescue the trafficking defect of full-length F508del-CFTR and attenuate its gating defect. We interpret these data to suggest that the solubilizing mutations utilized to facilitate F508del-NBD1 production also assist folding of full-length F508del-CFTR protein. Thus, the available crystal structure of F508del-NBD1 might correspond to a partially corrected conformation of this domain.

INTRODUCTION

The common life-shortening genetic disease cystic fibrosis (CF) is caused by mutations in the ATP-binding cassette (ABC) transporter, cystic fibrosis transmembrane conductance regulator (CFTR) (Rowe et al., 2005). Over 1500 CFTR gene variants have been described so far, most presumed to cause CF. However, one single mutation, the deletion of phenylalanine 508 (F508del), accounts for approximately 70% of all CF chromosomes worldwide (http://www.genet.sickkids.on.ca/cftr/).

CFTR is a Cl⁻ channel that is expressed at the apical membrane of epithelial cells, where it regulates fluid and electrolyte transport and is regulated by cAMP-dependent phosphorylation and cycles of ATP binding and hydrolysis (Cai et al., 2007). CFTR has a modular design composed of two membrane-spanning domains (MSDs) which form the channel pore, two cytoplasmic nucleotide-binding domains (NBDs) which regulate channel gating, and a unique cytoplasmic regulatory domain (RD), the phosphorylation of which regulates channel activity.

The most critical problem associated with the F508del mutation, which is located in NBD1, is its impaired folding, which prevents the mutant protein from acquiring a native conformation and trafficking to the cell membrane (Riordan, 2005). Hence, F508del-CFTR is recognized as misfolded and retained by endoplasmic reticulum (ER) quality control (ERQC), which targets F508del-CFTR for degradation by the ubiquitin-proteasomal pathway (UPP) (Vashist and Ng, 2004). Whereas almost all F508del-CFTR is targeted for degradation by the UPP, numerous studies have demonstrated that the mutant protein can mature under specific conditions, including incubation either at low temperature (Denning et al., 1992), with cellular osmolytes (Brown et al., 1996), or in the presence of second-site suppressors (Teem et al., 1993). Some function is restored by these manipulations, suggesting that a therapeutic strategy for CF based on enhancing the maturation of F508del-CFTR is possible.

A variety of studies have thus focused on understanding CFTR folding and structure so as to elucidate the molecular basis of CF. Recently, high-resolution structures of murine and human NBD1 have provided invaluable information about the structure of NBD1 (Lewis et al., 2004, 2005). Together with the atomic-resolution structures of other ABC transporters (Hollenstein et al., 2007), these NBD structures also provide insight into the putative interactions of NBD1 with other domains of CFTR.

To better understand, at a molecular level, how the F508del-CFTR mutation perturbs the structure of NBD1, Lewis et al. (2005) elucidated the crystal structure of F508del-NBD1. However, to promote domain solubilization and, hence, crystallization, Lewis et al. (2005) incorporated a series of mutations into the human NBD1 sequence. Some of these mutations represented sequence changes between human CFTR and CFTRs from other species, whereas others (G550E, R553Q, and R555K) had been previously identified as F508del-CFTR revertant mutations (Teem et al., 1996; deCarvalho et al., 2002; Chang et al., 1999). F508del-CFTR revertants are second-site mutations in *cis* with F508del which rescue the cell-surface expression and
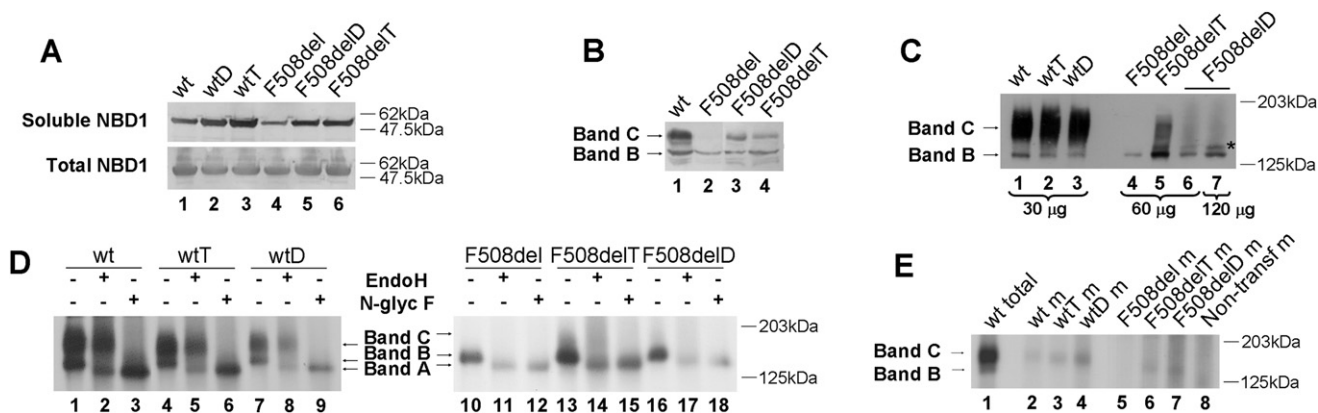
Figure 1. Biochemical Analysis of CFTR Variants

(A) Solubility of wt- and F508del-NBD1 in the absence and presence of solubilizing mutants. Soluble and total protein are shown for each NBD1 construct. Total NBD1 protein corresponds to one eighth of the loaded soluble sample.

(B) Western blotting of total protein extracts from HEK293 cells transiently transfected with pCMV-F508del-CFTR and solubilizing mutations as indicated, after treatment with sodium butyrate (5 mM) at 37°C for 48 hr (two independent transfections were made for each clone shown for the solubilizing mutants).

(C) WB of total protein (30 μg for wt, wtD, and wtT, 60 μg for F508del and F508delT, and 60 or 120 μg for F508delD) from BHK cells stably expressing wt- and F508del-CFTR in the absence and presence of solubilizing mutants. The asterisk identifies the band of intermediate mobility between bands B and C.

(D) Glycosidase analysis of the indicated CFTR variants stably expressed in BHK cells. Immunoprecipitated CFTR protein was treated with 500 U of either endoglycosidase H (endoH) or N-glycosidase F (N-glyc F). The minus and plus signs denote the absence and presence of glycosidases, respectively.

(E) Cell-surface biotinylation of CFTR variants stably expressed in BHK cells. Protein detected at the cell surface (m) is compared with total protein for wt-CFTR (total). For total wt-CFTR, loaded sample corresponds to a confluent 35 mm Petri dish. For membrane proteins, loaded samples correspond to either one confluent 60 mm Petri dish (cells expressing wt-, wtT-, and wtD-CFTR), three confluent 100 mm Petri dishes (F508del- and F508delT-CFTR or nontransfected cells), or two confluent T175 flasks (F508delD-CFTR). Numbers are used to identify individual samples, while labeled arrows indicate the positions of bands A, B, and C.

Cl⁻ channel function of F508del-CFTR. Of note, one of these revertants, R553Q, was found in an F508del-homozygous patient with mild CF disease (Dörk et al., 1991). In addition, another revertant mutation, G550E, likely acts by altering the structure of NBD1 (Roxo-Rosa et al., 2006). Examination of the structures of wt- and F508del-NBD1 revealed little or no structural changes besides deformation of the local surface topography around the F508 residue (Lewis et al., 2005). Based on these data and a substantial amount of biochemical, biophysical, and cell biological data, new hypotheses were then proposed (Chen et al., 2004; Thibodeau et al., 2005; Du et al., 2005; Cui et al., 2006). Because the F508 residue lies at a domain-domain interface, these hypotheses argue that altered domain-domain interactions, resulting from the F508del mutation, impact upon the global structure of CFTR. Furthermore, they suggest that impairment of these interdomain interactions is the fundamental defect associated with the F508del mutation. However, it remains plausible to envisage that a structure of F508del-NBD1 with more conformational differences than just those at the surface described by Lewis et al. (2005) would likely further disrupt such interdomain interactions, in particular those involving NBD1.

Because of the presence of F508del revertant mutations in the crystal structure of F508del-NBD1, further F508del-NBD1 structures were produced (Lewis, 2005) lacking known F508del revertants (http://www.rcsb.org/pdb/). However, these new F508del-NBD1 crystal structures still required either two (F494N/Q637R; Protein Data Bank [PDB] ID code: 2BBT) or three (F429S/F494N/Q637R; PDB ID code: 2BBS) additional mutations for domain solubility and, hence, crystal formation (Lewis, 2005).

Given the ability of solubilizing mutations to increase the yield of NBD1 and facilitate its crystallization (Lewis et al., 2005), we

hypothesized that these mutations might also promote the folding of both isolated NBD1 and full-length CFTR protein. To test these ideas, we investigated the effects of the mutations F494N/Q637R and F429S/F494N/Q637R on wt- and F508del-CFTR by studying: (1) the in vivo folding yield of NBD1, (2) the processing and trafficking of the full-length CFTR protein, and (3) the Cl⁻ channel function of CFTR. Our data reveal that solubilizing mutations attenuate the trafficking and gating defects of F508del-CFTR.

RESULTS

While studying the effects of F508del on the structure of NBD1 from CFTR, Lewis (2005) introduced the mutations F494N/Q637R (double; D) and F429S/F494N/Q637R (triple; T) into NBD1 to improve domain solubility and crystallization. To investigate whether these variants counteract the effects of F508del on protein processing and channel function, we performed three types of experiments. First, the yield of these NBD1 variants was tested when expressed in bacteria. Second, full-length CFTR folding and maturation were assessed in novel BHK cell lines stably expressing wt- and F508del-CFTR in *cis* with these mutations. Third, their effects on cell-surface expression and function were determined using biochemical and electrophysiological techniques.

Solubilizing Mutations Improve
wt- and F508del-NBD1 Yield

To explore whether F429S, F494N, and Q637R improve the yield of soluble NBD1, wt-NBD1 and F508del-NBD1 were expressed in bacterial cells in the absence and presence of the solubilizing mutations. Confirming the data of Lewis et al. (2005), Figure 1A

(lanes 4–6) demonstrates that F508delD- and F508delT-NBD1 generated greater amounts of soluble NBD1 than did F508del-NBD1. Interestingly, the data also indicate that F508delD- and F508delT-NBD1 had marginally higher folding yields than did wt-NBD1 (compare lane 1 to lanes 5 and 6) by 1.2- and 1.5-fold, respectively (the solubility of F508del-NBD1 was 0.6 that of wt-NBD1). Moreover, the soluble yields of wtD- and wtT-NBD1 were enhanced relative to that of wt (lanes 1–3) by 1.8- and 2.0-fold, respectively. These data thus confirm that the solubilizing mutations markedly increase the low yield of soluble F508del-NBD1.

Solubilizing Mutations Rescue F508del-CFTR from ER Mislocalization

When western blotting (WB) is used to investigate the processing of CFTR, two different forms of wt-CFTR protein are visualized: an immature core-glycosylated form that is found in the ER (150 kDa; band B) and a mature fully glycosylated form that has been processed through the Golgi apparatus and delivered to the cell membrane (170–180 kDa; band C) (Cheng et al., 1990). To investigate the processing of F508del-CFTR in *cis* with the double or triple solubilizing mutations, total protein extracts from HEK293 cells transiently transfected with F508del-, F508delD-, and F508delT-CFTR cDNAs were assessed by WB analysis using the anti-CFTR M3A7 antibody. To augment the expression of these CFTR constructs, cells were treated with sodium butyrate (5 mM) at 37°C for 24 hr (Cheng et al., 1995). Figure 1B demonstrates that some fraction of F508delD- and F508delT-CFTR (lanes 3 and 4) are processed to the mature form, whereas no measurable mature F508del-CFTR is observed (lane 2).

Butyrate has been reported to partially rescue the cell-surface expression of F508del-CFTR (Cheng et al., 1995). Therefore, the effects of solubilizing mutations on F508del-CFTR processing in the absence of butyrate were assessed by WB using novel BHK cell lines stably expressing wt- or F508del-CFTR in *cis* with the solubilizing mutations. Figure 1C (lanes 1–3) demonstrates that the solubilizing mutations only slightly affected the proportion of processed wt-CFTR at steady state (wt: 89 ± 7%, n = 5; wtD: 93 ± 3%, n = 3; wtT: 90 ± 2%, n = 3; where 100% corresponds to total CFTR in each sample, i.e., band B + band C). However, these mutations promoted the maturation of F508del-CFTR. F508delD- (Figure 1C, lanes 6 and 7) and especially F508delT-CFTR (Figure 1C, lane 5) generated higher molecular mass forms of CFTR, consistent with full glycosylation (band C), that were absent in F508del-CFTR (Figure 1C, lane 4). Of note, in addition to band C, a band of intermediate mobility (between bands B and C, marked with an asterisk in Figure 1C) was consistently detected in both F508delD- and F508delT-CFTR, which is absent in samples of wt-, wtD-, or wtT-CFTR.

To confirm the identity of the bands observed with F508delD- and F508delT-CFTR, we used endoglycosidase H (endoH) and N-glycosidase F (N-glyc F) to assess the glycosylation status of these CFTR variants. Like band C of wt-, wtT-, and wtD-CFTR (Figure 1D, lanes 3, 6, and 9), the higher molecular mass forms of F508delT- and F508delD-CFTR were sensitive to N-glyc F (Figure 1D, lanes 15 and 18) which, by removing glycans from bands B and C, convert CFTR to its bare polypeptidic chain (band A). However, the intermediate band of F508delT- and F508delD-CFTR was also sensitive to EndoH (Figure 1D, lanes 14 and 17), indicating that its glycosylation status is distinct from

that of band C of wt-CFTR. However, this intermediate band might correspond to a post-ER glycosylated form of CFTR, as it is also absent in F508del-CFTR samples (Figure 1C, lane 4).

To determine whether F508delD- and F508delT-CFTR are delivered to the plasma membrane, cell-surface biotinylation assays were performed using a modified nonpermeant biotin reagent that only binds (available) primary amines at the cell surface from the external milieu. Figure 1E (lanes 2–4) reveals that band C of wt-, wtD-, and wtT-CFTR were present at the cell surface. By contrast, F508del-CFTR could not be detected in the cell-surface fraction (lane 5), confirming the specificity of this method for identifying protein at the cell surface. For both F508delT-CFTR and F508delD-CFTR, processed forms previously detected by WB (Figure 1C, lanes 5–7) were also detected in the cell-membrane fraction, although in reduced amounts (lanes 6 and 7).

Solubilizing Mutations Restore Function to F508del-CFTR

To further confirm the presence of processed forms of F508delD- and F508delT-CFTR at the cell membrane, we analyzed CFTR function using the iodide efflux technique. This method assesses the activity of a large population of CFTR constructs at the surface of intact cells.

When BHK cells expressing F508del-CFTR were incubated at 37°C, they failed to generate an efflux of iodide (Figure 2A, open squares), whereas after 24 hr incubation at 26°C they exhibited a sustained efflux of iodide (Figure 2A, black squares), albeit 1.4-fold smaller and with slower onset and decay than the large transient efflux of iodide elicited by wt-CFTR at 37°C (Figure 2A, gray circles; Figure 2E). Figures 2B and 2E demonstrate that, at 37°C, solubilizing mutations were without effect on the efflux of iodide elicited by wt-CFTR. Indeed, neither the time course nor the magnitude of the response differed between wt-, wtD-, and wtT-CFTR (Figure 2B). Of note, at 37°C, both F508delD- (Figure 2C) and F508delT-CFTR (Figure 2D) generated effluxes of iodide with time courses similar to that of wt-CFTR but magnitudes comparable to that of low-temperature rescued F508del-CFTR (Figure 2E). Moreover, after incubation at 26°C, the magnitude and time courses of F508delD- (Figure 2C) and F508delT-CFTR (Figure 2D) iodide efflux were comparable to that of wt-CFTR at 37°C (Figure 2E).

Solubilizing Mutations Alter the Function of F508del-CFTR, but Not That of wt-CFTR

To learn whether solubilizing mutations alter the function of wt- and F508del-CFTR Cl⁻ channels, we used the excised inside-out configuration of the patch-clamp technique. Visual inspection of single-channel records (Figure 3A) demonstrates that the pattern of channel gating of low-temperature rescued F508del-CFTR, recorded at 37°C, differs strikingly from that of wt-CFTR. For F508del-CFTR, infrequent bursts of channel openings are separated by closed periods dramatically longer than those of wt-CFTR.

Figure 3 reveals that the solubilizing mutations were without effect on the function of wt-CFTR. wtD- and wtT-CFTR had the same current amplitude (i), open probability (P_o), mean burst duration (MBD), and interburst interval (IBI) as wt-CFTR (p > 0.1). By contrast, these mutations enhanced the P_o of F508del-CFTR
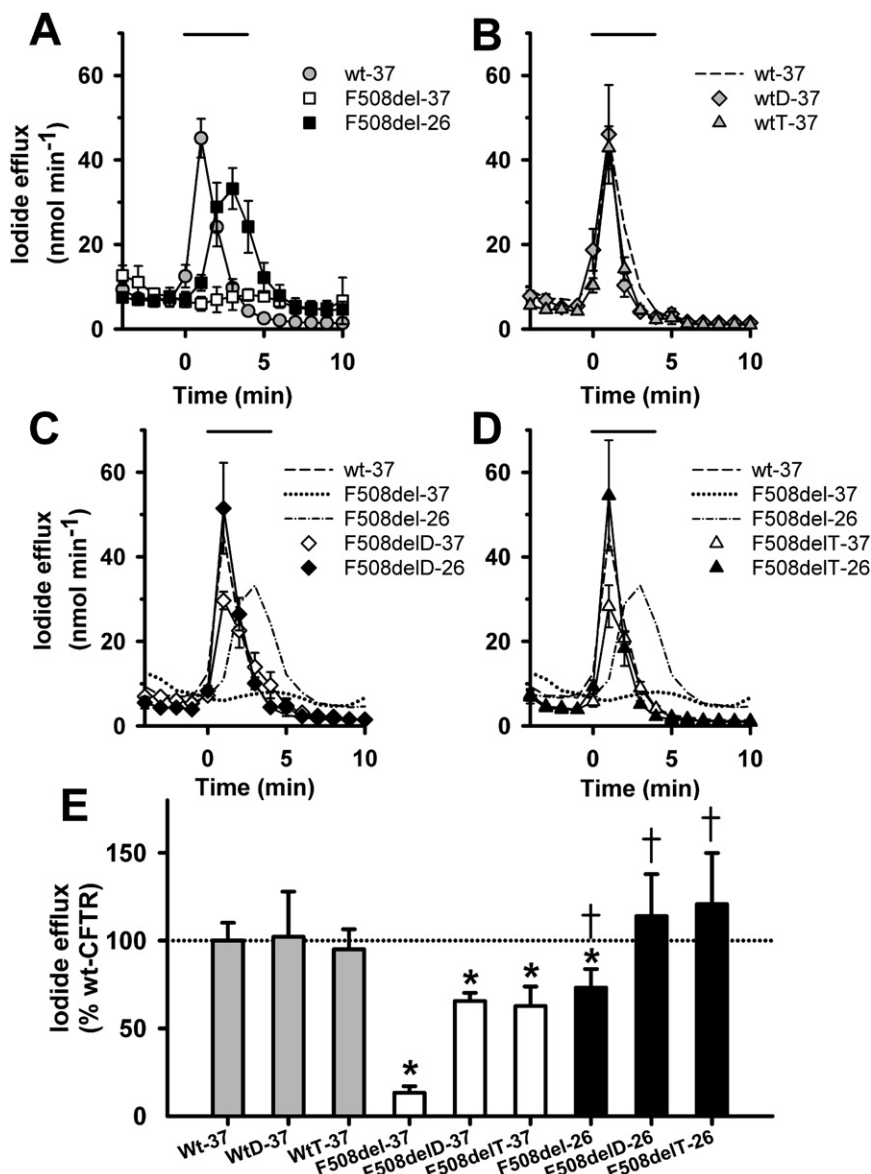
Figure 2. Iodide Efflux from BHK Cells Expressing Solubilizing Mutants

(A–D) Time courses of iodide efflux from BHK cells stably expressing the indicated CFTR variants cultured at either 37°C or 26°C. During the periods indicated by the bars, forskolin (10 μM) and genistein (50 μM) were present in the efflux buffer. Data are means (n = 4–9) at each point. Where not shown, error bars are smaller than symbol size.

(E) Magnitude of peak iodide efflux generated by different CFTR constructs expressed as a percentage of that of wt-CFTR. Asterisks indicate significant differences from wt-CFTR ($p < 0.05$), whereas crosses indicate significant differences between the same CFTR variants cultured at 37°C and 26°C ($p < 0.05$). Data are expressed as means ± SEM of $n \geq 4$ observations.

somal degradation (Ward et al., 1995; Jensen et al., 1995). Because F508del dramatically attenuates the folding yield of isolated NBD1 at different temperatures but has little effect on the measured stability of the folded domain (Qu and Thomas, 1996), the mutation likely affects an early step in CFTR folding by imposing a significant energy barrier between a folding intermediate and the native conformation or by decreasing the energy barrier for entering the off-pathway. Thus, the observation that solubilizing mutations enhance the yield of solubilized NBD1 (Lewis et al., 2005) suggests that these mutations might counteract the relative change in energy barrier imposed by F508del and, hence, improve NBD1 folding.

Understanding the alteration in biochemical and biophysical properties of full-length F508del-CFTR associated with the inclusion of NBD1 solubilizing mutations is important in several respects. First, the analysis and interpretation of the structures of F508del-NBD1 are potentially affected by the inclusion of these mutations. Second, investigating the coordinated role that multiple, nonadjacent sites to F508del play in a common, but complex, protein fold might help understanding the principal elements that define the F508del-NBD1 fold. Finally, recognizing the specific spatial constraints of F508del-NBD1 and pinpointing differences between it and wt-NBD1 might aid the design of molecules with therapeutic potential aimed at correcting such differences (Moran and Zegarra-Moran, 2005).

Solubilizing Mutations Attenuate F508del-CFTR Trafficking and Functional Defects

To determine how the double (D) and triple (T) solubilizing mutations of NBD1 impact on the folding of NBD1 and CFTR, we first evaluated their effects on the biochemical properties of NBD1 in vitro and then on the biochemical and functional properties
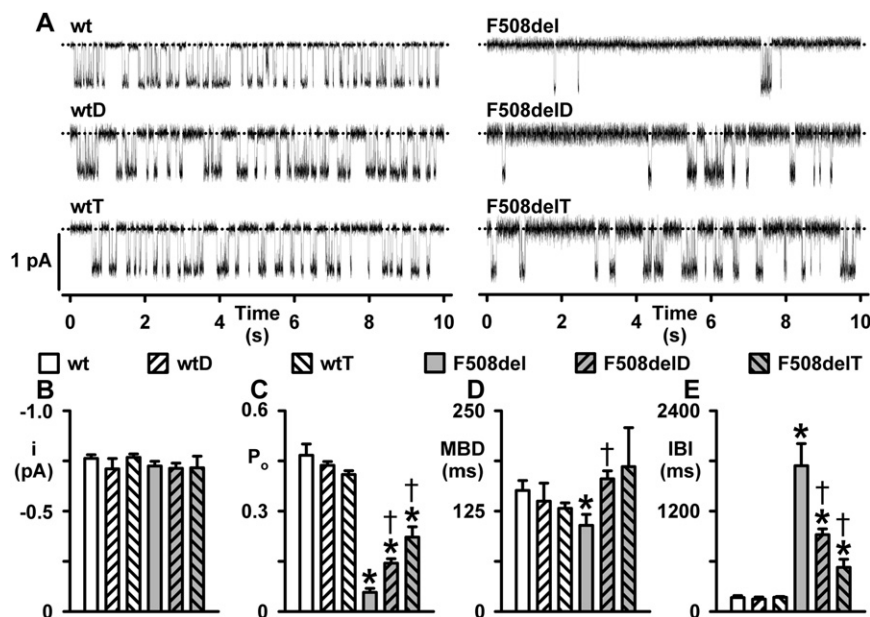
by altering channel gating (Figures 3A and 3C). Both mutations restored MBD to values equivalent to that of wt-CFTR (Figure 3D). Of note, they also attenuated markedly the prolonged IBI of F508del-CFTR (Figure 3E). F508delT-CFTR had the greatest effect, decreasing IBI from 10-fold longer than wt-CFTR to only 3-fold longer. As for wt-CFTR, the solubilizing mutations were without effect on the i of F508del-CFTR ($p > 0.5$), which was equivalent to that of wt-CFTR (Figure 3B). These data thus demonstrate that solubilizing mutations are without effect on the gating behavior of wt-CFTR but strongly attenuate the gating of F508del-CFTR.

DISCUSSION

The most common CF mutation, F508del, causes a temperature-sensitive folding defect that is recognized by the ERQC leading to the targeting of newly synthesized F508del-CFTR for protea-

Figure 3. Single-Channel Currents of wt- and F508del-CFTR in the Absence and Presence of Solubilizing Mutants

(A) Representative single-channel recordings of the indicated CFTR variants in excised inside-out membrane patches from BHK cells. ATP (1 mM) and PKA (75 nM) were continuously present in the intracellular solution; voltage was −50 mV, and there was a Cl$^-$ concentration gradient across the membrane ([Cl$^-$]$_{int}$, 147 mM; [Cl$^-$]$_{ext}$, 10 mM). Dashed lines indicate the closed channel state and downward deflections correspond to channel openings.

(B–E) Single-channel current amplitude (i), open probability (P$_o$), mean burst duration (MBD), and interburst interval (IBI) of the indicated CFTR variants. Columns and error bars are means ± SEM (wt: i, n = 4, P$_o$, MBD, IBI, n = 7; wtD: i, P$_o$, n = 7, MBD and IBI, n = 3; wtT: i, P$_o$, n = 4, MBD and IBI, n = 3; F508del: n = 7 for all data; F508delD: n = 6 for all data; F508delT: n = 4 for all data). The asterisks and crosses indicate values that are significantly different from those of wt- (p < 0.05) and F508del-CFTR (p < 0.05), respectively. For wt-CFTR, C127 cells were used to determine P$_o$, MBD, and IBI because these cells express low levels of CFTR protein, whereas BHK cells were used to determine i. However, in one single-channel patch from a BHK cell expressing wt-CFTR, values of i, P$_o$, MBD, and IBI did not differ from those obtained using C127 cells expressing wt-CFTR. For F508del, F508delD, and F508delT, values of MBD and IBI calculated using multichannel patches did differ from those acquired using single-channel patches.

of full-length CFTR in vivo. Consistent with the data of Lewis et al. (Lewis et al., 2005; Lewis, 2005), the solubilizing mutations dramatically enhanced the yield of soluble NBD1 produced in *Escherichia coli*, independent of total protein expression for both wt- and F508del-NBD1. Of note, the yield of F508del-NBD1 with solubilizing mutations was even higher than that of wt-NBD1 without the solubilizing mutations.

Moreover, when introduced into full-length CFTR, the solubilizing mutations partially restored the maturation of F508del-CFTR, as seen by the appearance of band C. These data indicate that solubilizing mutations allow at least some F508del-CFTR to exit the ER and traffic through the Golgi apparatus. However, the amounts of processed F508delT-CFTR and especially F508delD-CFTR were significantly less than that of wt-CFTR.

Interestingly, in addition to bands B and C, a band of intermediate mobility was observed for both F508delD- and F508delT-CFTR. Susceptibility to endoH confirmed that this intermediate band does not acquire the same state as wt-CFTR. This higher molecular weight form of F508del-CFTR might correspond to incompletely processed CFTR structures, probably lacking the final glycan residues (e.g., fucose and/or sialic acid) (Hammerle et al., 2000) which appear to be stabilized by the solubilizing mutations. Because single-chain glycosylated forms of CFTR are endoH resistant like those of wt-CFTR (Hammerle et al., 2000), we consider it unlikely that CFTR variants containing solubilizing mutations possess just one, instead of two, glycan chains. Nevertheless, partially glycosylated forms of CFTR would be expected to be functional at the cell membrane, because glycosylation null CFTR mutants form regulated Cl$^-$ channels (Chang et al., 1994; Farinha and Amaral, 2005). It is possible to envisage that this intermediate band also occurs transiently during processing of wt-CFTR, but is rapidly converted into the fully pro-

cessed form and thus is not detected. Interestingly, we have recently observed it (or a similar form) under general inhibition of protein kinases (Schmidt et al., 2008).

Data from cell-surface biotinylation demonstrate that the band C observed for the F508delD- and F508delT-CFTR variants is present at the cell surface, albeit in reduced amounts compared to that for wt-CFTR. Confirmation that both F508delD- and F508delT-CFTR are present at the membrane was provided by functional studies using iodide efflux and patch-clamp techniques. By contrast, and as widely described, cAMP agonists failed to elicit an efflux of iodide from cells expressing F508del-CFTR at 37°C.

Studies of the single-channel activity of F508delD and F508delT revealed that they had MBD values similar to wt-CFTR. Using the ATP-driven NBD dimerization model of CFTR channel gating (Vergani et al., 2005), these data suggest that the solubilizing mutations might stabilize the NBD dimer of CFTR. However, because the IBI values of F508delD- and F508delT-CFTR are still greater than that of wt-CFTR, it is likely that the energy barrier for channel opening remains greater than that for wt-CFTR. Nevertheless, our data suggest that the solubilizing mutations accelerate markedly NBD dimerization compared with that of F508del-CFTR.

Taken together, these data indicate that the solubilizing mutations partially rescue the trafficking defect and restore some function to F508del-CFTR. Interestingly, iodide efflux from cells expressing the F508delD-CFTR and F508delT-CFTR variants was augmented by low-temperature incubation, indicating that the effects of solubilizing mutations and low temperature on F508del-CFTR trafficking and function are additive. This suggests that solubilizing mutations and low temperature might rescue F508del-CFTR by distinct mechanisms.

Structural Implications

An interesting aspect of the action of the solubilizing mutations (double, F494N/Q637R; triple, F429S/F494N/Q637R) is their remote location from that of F508. Based on this consideration, Lewis et al. (2005) speculated that these mutations would not influence the structure of hNBD1. However, the effect produced by F494N is not completely unexpected, as structural crosstalk between the side chain of the F508 residue (e.g., F508R) and the Q loop or γ-phosphate switch (e.g., residues W496 and M498) has been previously shown to occur (Massiah et al., 1999).

Interestingly, the C terminus of the crystal structure of NBD1 contains a long α helix (H9b) that is not present in the crystal structures of NBDs from other ABC transporters (Lewis et al., 2004). Curiously, Q637R lies in this helix, known as the RD1 region (residues 590–672) of NBD1. This region was initially considered to be within the R domain (Riordan et al., 1989), but is now regarded to be part of NBD1 based on amino acid sequence analysis and functional studies (Dulhanty and Riordan, 1994; Bianchet et al., 1997; Chan et al., 2000). Structural and experimental evidence argue that helix H9b is either an integral component of the NBD1 fold or a more "loose" structural element that is highly favorable for the folding of this domain (Lewis et al., 2004). In support of this notion, our data indicate that Q637R, at least with one additional solubilizing mutation (F494N), might contribute to the increased solubility of F508del-NBD1 and to the partial rescue of F508del-CFTR trafficking and function.

The third solubilizing mutation, F429S, further promotes the revertant effect produced by the double mutant (F494N/Q637R) on F508del-CFTR, as the triple mutant (F429S/F494N/Q637R) visibly increased maturation of F508del-CFTR as measured by the higher maturation yield at steady state of F508delT-CFTR compared with that of F508delD-CFTR (Figure 1C). The F429 residue occurs in an insertion (406–434), between the first (393–400) and second (441–448) β strands of NBD1, which was found to be disordered in NBD1 crystals (Ostedgaard et al., 2000). This suggests that F429S might lie on the surface of NBD1 in a position where it likely interacts with the environment (Lewis et al., 2004, 2005).

Comparison with Other Revertants

Using the same cellular system employed to investigate the solubilizing mutations, we recently examined the mechanism of action of two other F508del-CFTR revertants, G550E and 4RK, the simultaneous mutation of four arginine-framed tripeptides (AFTs), R29K, R516K, R555K, and R766K (Roxo-Rosa et al., 2006). We suggested that these mutations partially rescue F508del-CFTR by distinct mechanisms. G550E likely alters the conformation of NBD1, whereas 4RK allows F508del-CFTR to escape endoplasmic reticulum retention/retrieval mediated by AFTs. We also showed that both G550E and 4RK affected wt-CFTR (Roxo-Rosa et al., 2006). By contrast, the present results demonstrate that solubilizing mutations attenuate markedly both the trafficking and functional defects of F508del-CFTR without, however, affecting wt-CFTR.

Moreover, whereas the revertants 4RK and G550E restored the iodide efflux of F508del-CFTR to wt levels (Roxo-Rosa et al., 2006), the magnitude of iodide efflux elicited by F508delD- and F508delT-CFTR was less than that of wt-CFTR. This indicates that the solubilizing mutations are not as effective as 4RK and G550E at augmenting either the cell-surface expres-

sion or function of F508del-CFTR. However, at steady state, F508delD and F508delT produced amounts of band C similar to those of G550E- or 4RK-F508del (present study and A.S. and M.D.A., unpublished data). Thus, the surface levels of F508del-CFTR rescued by different genetic variants do not strictly correlate with the overall activity of F508del-CFTR as a Cl⁻ channel. Altogether, these data argue that different genetic variants have distinct effects on the trafficking and function of F508del-CFTR.

Moreover, analysis of CFTR channel gating revealed that the NBD1 solubilizing mutations analyzed here restored the attenuated MBD of F508del-CFTR to wt-CFTR levels and attenuated dramatically the greatly prolonged IBI of F508del-CFTR. By contrast, both revertant mutations markedly prolonged the MBD of F508del-CFTR, with G550E exceeding that of wt-CFTR by 4-fold (Roxo-Rosa et al., 2006). Moreover, only G550E suppressed the prolonged IBI of F508del-CFTR (Roxo-Rosa et al., 2006), reducing it to a level similar to that achieved here with F508delT-CFTR. We interpret these data to suggest that the conformation state(s) that solubilizing mutations achieve is closer to that of wt-CFTR than the conformation produced by the revertant G550E (Roxo-Rosa et al., 2006).

Consistent with this interpretation, the revertants, especially G550E, extended the MBD and elevated the P_o of wt-CFTR (Roxo-Rosa et al., 2006), whereas wt-CFTR containing the solubilizing mutations had the same MBD, IBI, and P_o as wt-CFTR. We thus suggest that the solubilizing mutations act specifically on F508del-CFTR (in contrast to G550E) to abrogate its gating defect, possibly through correction of NBD1 and/or CFTR folding. Hence, the conformation of F508del-CFTR containing solubilizing mutations is markedly different from that achieved by low-temperature correction, which fails to rescue the gating defect of F508del-CFTR (Denning et al., 1992).

In conclusion, our data suggest that a crystal structure of F508del-NBD1 without solubilizing mutations is required to determine whether and how the F508del mutation perturbs the structure of this domain. Meanwhile, it is plausible to envisage that the F508del mutation per se alters the properties of NBD1 and, hence, also the interaction of NBD1 with other domains of CFTR. Finally, solubilizing mutations are attractive sites to target for the design of small-molecule CFTR correctors to treat CF.

SIGNIFICANCE

F508del, the most frequent mutation in CF, disrupts both the trafficking and channel gating of CFTR. The available crystal structure of F508del-NBD1 was determined after the introduction of additional mutations (F494N/Q637R or F429S/F494N/Q637R) to help domain solubilization and crystal formation. Whereas comparison of this structure with that of wild-type NBD1 revealed only minor conformational changes, the present study demonstrates that these solubilizing mutations partially rescue in vivo both the trafficking and functional defects of full-length F508del-CFTR. These data suggest that the existing crystal structure of F508del-NBD1 is that of a partially corrected conformation and that the structure of F508del-NBD1 without additional mutations is still needed to gain further insight into how the F508del-NBD1 differs from wt-NBD1.

EXPERIMENTAL PROCEDURES

Solubility of CFTR-NBD1

His-tagged hNBD1s (amino acids 388–677) containing different CFTR-NBD1 variants were cloned into the pET-SUMO vector and expressed in bacterial BL21 cells at 15°C after IPTG induction as described previously (Thibodeau et al., 2005). Total NBD1 was obtained from sonicated whole-cell lysates and soluble NBD1 from the supernatant of a 30,000 × g centrifugation. Samples were run on 10% (w/v) Tris-tricine SDS-PAGE gels, transferred to nitrocellulose membranes, and probed with an anti-His monoclonal antibody and an anti-mouse HRP-labeled secondary antibody. Total NBD1 samples correspond to one eighth of the loaded soluble samples.

Site-Directed Mutagenesis, Cells, and CFTR Expression

To introduce the solubilizing mutations F494N/Q637R and F429S/F494N/Q637R into wt- and F508del-CFTR cDNAs in the pNUT expression vector, we used the primers F429S, 5′-GGTGATGACAGCCTCTCCTTCAGTAATTTCTCA-3′; F494N, 5′-CATTCTGTTCTCAGAATTCCTGGATTATGCCTGG-3′; Q637R, 5′-GAACTCCAAAATCTAAGGCCAGACTTTAGCTC-3′ and the Quik-Change site-directed mutagenesis kit (Stratagene). The identity of each solubilizing mutation was verified by sequencing.

For transient expression, HEK293 cells were transfected with 1.5 μg DNA of the pCMV-CFTR-Not6.2 construct containing different CFTR variants using Fugene6 (Roche). Twenty-four hours posttransfection, sodium butyrate (5 mM) was added for a further 24 hr to enhance CFTR expression.

To generate cell lines stably expressing high levels of CFTR variants, baby hamster kidney (BHK) cells were transfected with CFTR cDNAs (1.5 μg) using Lipofectin (Invitrogen) and selected for stable transfectants using methotrexate (500 μM). Cell lines expressing different solubilizing mutations are referred to as follows: wtD-CFTR, F494N-Q637R-CFTR; F508delD-CFTR, F494N-F508del-Q637R-CFTR; wtT-CFTR, F429S-F494N-Q637R-CFTR; and F508delT-CFTR, F429S-F494N-F508del-Q637R-CFTR. For each CFTR variant, seven BHK clones were analyzed by western blotting (WB). Of these, the clone expressing the highest level of CFTR protein was selected for further analyses, ensuring that CFTR expression levels among the different CFTR variants were equivalent. Cells were cultured, seeded, and used as described previously (Roxo-Rosa et al., 2006). In some experiments (see figure legends), cell-surface expression of F508del-CFTR variants was enhanced by incubating cells at 26°C for 24 hr.

Biochemical Analyses of CFTR Protein

To assay for CFTR protein expression by WB, cells expressing CFTR variants were lysed and extracts were analyzed as described (Farinha et al., 2004a) using the anti-CFTR monoclonal antibody M3A7 (Chemicon). Densitometry was performed as described previously (Farinha et al., 2004a).

Glycosidase Assays

Cells were metabolically labeled with [^{35}S]methionine and lysed prior to CFTR immunoprecipitation with the anti-CFTR monoclonal antibody M3A7 (Chemicon) as previously described (Farinha et al., 2004a). Immunoprecipitated CFTR was then incubated with 500 U endoglycosidase H (endoH) and N-glycosidase F (N-glyc F), both from New England Biolabs for 18 hr at 37°C as described (Farinha et al., 2004b). After digestion, samples were analyzed by electrophoresis followed by fluorography as described previously (Farinha et al., 2004a).

Cell-Surface Biotinylation

To determine the membrane-localized fraction of CFTR variants, cell-surface biotinylation was performed (Farinha et al., 2004b). Briefly, cells were cooled to 4°C, washed with phosphate-buffered saline (PBS), and labeled with 1 mg/ml sulfo-NHS-LC-biotin (Pierce). Labeled cells were lysed in 1 ml of RIPA buffer containing a cocktail of protease inhibitors. After biotinylation and lysis, samples were subjected to CFTR immunoprecipitation with the M3A7 antibody (Chemicon) and protein G agarose and then recaptured with avidin-Sepharose beads (Pierce). For total protein, CFTR was eluted, whereas for membranar proteins, samples were eluted using Laemmli sample buffer without bromophenol blue and diluted in RIPA buffer 10-fold, and the biotinylated fraction was captured using avidin-Sepharose beads (Pierce). Both total

CFTR and biotinylated CFTR were then in vitro phosphorylated by PKA (Promega) using [γ-^{32}P]ATP (New England Nuclear) and analyzed by SDS-PAGE.

Iodide Efflux Technique

CFTR-mediated iodide efflux was measured at room temperature as described (Lansdell et al., 1998) using the cAMP agonist forskolin (10 μM) and the CFTR potentiator genistein (50 μM; Sigma-Aldrich). Prior to commencing experiments, BHK cells were incubated for 1 hr in loading buffer containing 136 mM NaI, 3 mM KNO$_3$, 2 mM Ca(NO$_3$)$_2$, 20 mM HEPES, and 11 mM glucose (pH 7.4), with 1 M NaOH (osmolarity, 299 ± 0.48 mOsm; n = 36), and then washed thoroughly with efflux buffer (136 mM NaNO$_3$ replacing 136 mM NaI in the loading buffer; osmolarity, 291 ± 0.24 mOsm; n = 60). The amount of iodide in each sample of efflux buffer was determined using an iodide-selective electrode (MP225; Thermo Electron). Data are expressed as means ± SEM (standard error of the mean) of n observations; statistical analyses were performed using Student's t test, with a value of $p < 0.05$ considered statistically significant.

Electrophysiology

CFTR Cl$^-$ channels were recorded in excised inside-out membrane patches from BHK cells expressing CFTR constructs stably (wt-, wtD-, wtT-, and F508del-CFTR) or transiently (F508delD- and F508delT-CFTR). For wt-, wtT-, F508delD-, and F508delT-CFTR, cells were incubated at 37°C prior to study, whereas F508del-CFTR expressing cells were incubated at 28°C. Data were acquired and analyzed using an Axopatch 200B patch-clamp amplifier and pCLAMP (version 9.2) software (both from Molecular Devices) as described (Cai et al., 2006). The pipette (extracellular) solution contained 140 mM N-methyl-D-glucamine (NMDG), 140 mM aspartic acid, 5 mM CaCl$_2$, 2 mM MgSO$_4$, and 10 mM 2-([2-hydroxy-l,l-bis(hydroxymethyl)ethyl]amino)-ethane-sulfonic acid (TES) (pH 7.3), with Tris ([Cl$^-$], 10 mM). The bath (intracellular) solution contained 140 mM NMDG, 3 mM MgCl$_2$, 1 mM CsEGTA, and 10 mM TES (pH 7.3), with HCl ([Cl$^-$], 147 mM; [Ca^{2+}]$_{free}$, < 10^{-8} M) and was maintained at 37°C. To activate and sustain channel activity, PKA (75 nM) and ATP (1 mM) were added to all intracellular solutions; voltage was −50 mV. The number of active channels was determined based on the maximum number of simultaneous channel openings using the strategies described in Cai et al. (2006) to minimize errors when counting the number of active channels. Data were analyzed as described previously (Cai et al., 2006) and are expressed as means ± SEM of n observations, where n is the number of excised membrane patches; statistical analyses were performed using Student's unpaired t test, with a value of $p < 0.05$ considered statistically significant.

REFERENCES

Bianchet, M.A., Ko, Y.H., Amzel, L.M., and Pedersen, P.L. (1997). Modeling of nucleotide binding domains of ABC transporter proteins based on a F1-AT-Pase/recA topology: structural model of the nucleotide binding domains of the cystic fibrosis transmembrane conductance regulator (CFTR). J. Bioenerg. Biomembr. *29*, 503–524.

Brown, C.R., Hong-Brown, L.Q., Biwersi, J., Verkman, A.S., and Welch, W.J. (1996). Chemical chaperones correct the mutant phenotype of the delta F508 cystic fibrosis transmembrane conductance regulator protein. Cell Stress Chaperones *1*, 117–125.

Cai, Z., Taddei, A., and Sheppard, D.N. (2006). Differential sensitivity of the cystic fibrosis (CF)-associated mutants G551D and G1349D to potentiators of the cystic fibrosis transmembrane conductance regulator (CFTR) Cl⁻ channel. J. Biol. Chem. 281, 1970–1977.

Cai, Z., Chen, J.-H., Hughes, L.K., and Li, H. (2007). The physiology and pharmacology of the CFTR Cl⁻ channel. In Chloride Movements across Cellular Membranes, M. Pusch, ed. (San Diego: Elsevier Limited), pp. 109–143.

Chan, K.W., Csanady, L., Seto-Young, D., Nairn, A.C., and Gadsby, D.C. (2000). Severed molecules functionally define the boundaries of the cystic fibrosis transmembrane conductance regulator's NH2-terminal nucleotide binding domain. J. Gen. Physiol. 116, 163–180.

Chang, X.B., Hou, Y.X., Jensen, T.J., and Riordan, J.R. (1994). Mapping of cystic fibrosis transmembrane conductance regulator membrane topology by glycosylation site insertion. J. Biol. Chem. 269, 18572–18575.

Chang, X.B., Cui, L., Hou, Y.X., Jensen, T.J., Aleksandrov, A.A., Mengos, A., and Riordan, J.R. (1999). Removal of multiple arginine-framed trafficking signals overcomes misprocessing of delta F508 CFTR present in most patients with cystic fibrosis. Mol. Cell 4, 137–142.

Chen, E.Y., Bartlett, M.C., Loo, T.W., and Clarke, D.M. (2004). The deltaF508 mutation disrupts packing of the transmembrane segments of the cystic fibrosis transmembrane conductance regulator. J. Biol. Chem. 279, 39620–39627.

Cheng, S.H., Gregory, R.J., Marshall, J., Paul, S., Souza, D.W., White, G.A., O'Riordan, C.R., and Smith, A.E. (1990). Defective intracellular transport and processing of CFTR is the molecular basis of most cystic fibrosis. Cell 63, 827–834.

Cheng, S.H., Fang, S.L., Zabner, J., Marshall, J., Piraino, S., Schiavi, S.C., Jefferson, D.M., Welsh, M.J., and Smith, A.E. (1995). Functional activation of the cystic fibrosis trafficking mutant delta F508-CFTR by overexpression. Am. J. Physiol. 268, L615–L624.

Cui, L., Aleksandrov, L., Hou, Y.X., Gentzsch, M., Chen, J.H., Riordan, J.R., and Aleksandrov, A.A. (2006). The role of cystic fibrosis transmembrane conductance regulator phenylalanine 508 side chain in ion channel gating. J. Physiol. 572, 347–358.

deCarvalho, A.C.V., Gansheroff, L.J., and Teem, J.L. (2002). Mutations in the nucleotide binding domain 1 signature motif region rescue processing and functional defects of cystic fibrosis transmembrane conductance regulator delta F508. J. Biol. Chem. 277, 35896–35905.

Denning, G.M., Anderson, M.P., Amara, J.F., Marshall, J., Smith, A.E., and Welsh, M.J. (1992). Processing of mutant cystic fibrosis transmembrane conductance regulator is temperature-sensitive. Nature 358, 761–764.

Dörk, T., Wulbrand, U., Richter, T., Neumann, T., Wolfes, H., Wulf, B., Maass, G., and Tümmler, B. (1991). Cystic fibrosis with three mutations in the cystic fibrosis transmembrane conductance regulator gene. Hum. Genet. 87, 441–446.

Du, K., Sharma, M., and Lukacs, G.L. (2005). The deltaF508 cystic fibrosis mutation impairs domain-domain interactions and arrests post-translational folding of CFTR. Nat. Struct. Mol. Biol. 12, 17–25.

Dulhanty, A.M., and Riordan, J.R. (1994). A two-domain model for the R domain of the cystic fibrosis transmembrane conductance regulator based on sequence similarities. FEBS Lett. 343, 109–114.

Farinha, C.M., and Amaral, M.D. (2005). Most F508del-CFTR is targeted to degradation at an early folding checkpoint and independently of calnexin. Mol. Cell. Biol. 25, 5242–5252.

Farinha, C.M., Mendes, F., Roxo-Rosa, M., Penque, D., and Amaral, M.D. (2004a). A comparison of 14 antibodies for the biochemical detection of the cystic fibrosis transmembrane conductance regulator protein. Mol. Cell. Probes 18, 235–242.

Farinha, C.M., Penque, D., Roxo-Rosa, M., Lukacs, G., Dormer, R., McPherson, M., Pereira, M., Bot, A.G., Jorna, H., Willemsen, R., et al. (2004b). Biochemical methods to assess CFTR expression and membrane localization. J. Cyst. Fibros. 3 (Suppl 2), 73–77.

Hammerle, M.M., Aleksandrov, A.A., Chang, X.B., and Riordan, J.R. (2000). A novel CFTR disease-associated mutation causes addition of an extra N-linked oligosaccharide. Glycoconj. J. 17, 807–813.

Hollenstein, K., Dawson, R.J., and Locher, K.P. (2007). Structure and mechanism of ABC transporter proteins. Curr. Opin. Struct. Biol. 17, 412–418.

Jensen, T.J., Loo, M.A., Pind, S., Williams, D.B., Goldberg, A.L., and Riordan, J.R. (1995). Multiple proteolytic systems, including the proteasome, contribute to CFTR processing. Cell 83, 129–135.

Lansdell, K.A., Delaney, S.J., Lunn, D.P., Thomson, S.A., Sheppard, D.N., and Wainwright, B.J. (1998). Comparison of the gating behaviour of human and murine cystic fibrosis transmembrane conductance regulator Cl⁻ channels expressed in mammalian cells. J. Physiol. 508, 379–392.

Lewis, H. (2005). Structures of human CFTR NBD1 confirm conservation of the domain structure despite the delF508 mutation. Pediatr. Pulmonol. 40, 190–191.

Lewis, H.A., Buchanan, S.G., Burley, S.K., Conners, K., Dickey, M., Dorwart, M., Fowler, R., Gao, X., Guggino, W.B., Hendrickson, W.A., et al. (2004). Structure of nucleotide-binding domain 1 of the cystic fibrosis transmembrane conductance regulator. EMBO J. 23, 282–293.

Lewis, H.A., Zhao, X., Wang, C., Sauder, J.M., Rooney, I., Noland, B.W., Lorimer, D., Kearins, M.C., Conners, K., Condon, B., et al. (2005). Impact of the deltaF508 mutation in first nucleotide-binding domain of human cystic fibrosis transmembrane conductance regulator on domain folding and structure. J. Biol. Chem. 280, 1346–1353.

Massiah, M.A., Ko, Y.H., Pedersen, P.L., and Mildvan, A.S. (1999). Cystic fibrosis transmembrane conductance regulator: solution structures of peptides based on the Phe508 region, the most common site of disease-causing deltaF508 mutation. Biochemistry 38, 7453–7461.

Moran, O., and Zegarra-Moran, O. (2005). A quantitative description of the activation and inhibition of CFTR by potentiators: genistein. FEBS Lett. 579, 3979–3983.

Ostedgaard, L.S., Baldursson, O., Vermeer, D.W., Welsh, M.J., and Robertson, A.D. (2000). A functional R domain from cystic fibrosis transmembrane conductance regulator is predominantly unstructured in solution. Proc. Natl. Acad. Sci. USA 97, 5657–5662.

Qu, B.H., and Thomas, P.J. (1996). Alteration of the cystic fibrosis transmembrane conductance regulator folding pathway. J. Biol. Chem. 271, 7261–7264.

Riordan, J.R. (2005). Assembly of functional CFTR chloride channels. Annu. Rev. Physiol. 67, 701–718.

Riordan, J.R., Rommens, J.M., Kerem, B., Alon, N., Rozmahel, R., Grzelczak, Z., Zielenski, J., Lok, S., Plavsic, N., and Chou, J.L. (1989). Identification of the cystic fibrosis gene: cloning and characterization of complementary DNA. Science 245, 1066–1073.

Rowe, S.M., Miller, S., and Sorscher, E.J. (2005). Cystic fibrosis. N. Engl. J. Med. 352, 1992–2001.

Roxo-Rosa, M., Xu, Z., Schmidt, A., Neto, M., Cai, Z., Soares, C.M., Sheppard, D.N., and Amaral, M.D. (2006). Revertant mutants G550E and 4RK rescue cystic fibrosis mutants in the first nucleotide-binding domain of CFTR by different mechanisms. Proc. Natl. Acad. Sci. USA 103, 17891–17896.

Schmidt, A., Hughes, L.K., Cai, Z., Mendes, F., Li, H., Sheppard, D.N., and Amaral, M.D. (2008). Prolonged treatment of cells with genistein modulates the expression and function of the cystic fibrosis transmembrane conductance regulator. Br. J. Pharmacol., in press.

Teem, J.L., Berger, H.A., Ostedgaard, L.S., Rich, D.P., Tsui, L.C., and Welsh, M.J. (1993). Identification of revertants for the cystic fibrosis delta F508 mutation using STE6-CFTR chimeras in yeast. Cell 73, 335–346.

Teem, J.L., Carson, M.R., and Welsh, M.J. (1996). Mutation of R555 in CFTR-delta F508 enhances function and partially corrects defective processing. Receptors Channels 4, 63–72.

Thibodeau, P.H., Brautigam, C.A., Machius, M., and Thomas, P.J. (2005). Side chain and backbone contributions of Phe508 to CFTR folding. Nat. Struct. Mol. Biol. 12, 10–16.

Vashist, S., and Ng, D.T. (2004). Misfolded proteins are sorted by a sequential checkpoint mechanism of ER quality control. J. Cell Biol. 165, 41–52.

Vergani, P., Lockless, S.W., Nairn, A.C., and Gadsby, D.C. (2005). CFTR channel opening by ATP-driven tight dimerization of its nucleotide-binding domains. Nature 433, 876–880.

Ward, C.L., Omura, S., and Kopito, R.R. (1995). Degradation of CFTR by the ubiquitin-proteasome pathway. Cell 83, 121–127.